

## BIOLOGY CONTRIBUTION

# Experimental Investigation of Hematological Toxicity After Radiation Therapy Combined With Immune Checkpoint Inhibitors



Vincent R. Timnik,<sup>a,1</sup> Andreas Zoeschg,<sup>a,1</sup> Sarah Diederich, MSc,<sup>a</sup> Sophie M. Nefzger, BSc,<sup>a</sup> Ziyi Huang, MCM,<sup>a</sup> Nicole A. Schmid, MSc,<sup>a</sup> Maximilian Giller,<sup>a</sup> Katja Steiger, DVM,<sup>b,c</sup> Stephanie E. Combs, MD,<sup>a,c,d</sup> Guido Kroemer, PhD,<sup>e,f,g</sup> Thomas E. Schmid, PhD,<sup>a,d</sup> and Julius C. Fischer, MD<sup>a,e,f</sup>

<sup>a</sup>Department of Radiation Oncology, Klinikum rechts der Isar, TUM School of Medicine and Health, Technical University of Munich, Munich, Germany; <sup>b</sup>Comparative Experimental Pathology (CEP), Institute of Pathology, School of Medicine, Technical University of Munich, Munich, Germany; <sup>c</sup>German Cancer Consortium (DKTK), Partner-site Munich and German Cancer Research Center (DKFZ), Heidelberg, Germany; <sup>d</sup>Helmholtz Zentrum München, Institute of Radiation Medicine, Neuherberg, Germany; <sup>e</sup>Centre de Recherche des Cordeliers, Equipe labellisée par la Ligue contre le cancer, Université Paris Cité, Sorbonne Université, Inserm U1138, Institut Universitaire de France, Paris, France; <sup>f</sup>Metabolomics and Cell Biology Platforms, Gustave Roussy Cancer Center, Université Paris Saclay, Villejuif, France; and <sup>g</sup>Institut du Cancer Paris CARPEM, Hôpital Européen Georges Pompidou, France-HP, Paris, France

Received Oct 28, 2024; Revised Feb 28, 2025; Accepted for publication Apr 5, 2025

Corresponding author: Julius C. Fischer, MD; E-mail: [Julius.fischer@tum.de](mailto:Julius.fischer@tum.de)

Author Responsible for Statistical Analyses: Julius C. Fischer, MD; E-mail: [Julius.fischer@tum.de](mailto:Julius.fischer@tum.de)

Vincent R. Timnik and Andreas Zoeschg made equal contributions to this study.

Disclosures: S.E.C.: Consulting fees from Icotec AG (Switzerland), HMG Systems Engineering GmbH (Germany), Bristol Myers Squibb BMS (Germany); payment or honoraria for lectures, presentations, speakers bureaus, manuscript writing, or educational events (most speaking appointments include reimbursement of travel costs – does not apply for virtual appointments): Roche, BMS, Brainlab, AstraZeneca, Accuray, Dr Sennewald, Daiichi Sankyo, Elekta, Medac, and med update GmbH. K.S. has received reimbursement for travel costs from Akoya Biosciences and 10x Genomics, and is a member of the TRIMT GmbH advisory board. G.K. is on the Board of Directors of the Bristol Myers Squibb Foundation France. G.K. is a scientific cofounder of everImmune, Osasuna Therapeutics, Samson Therapeutics, and Therafast Bio. G.K. is on the scientific advisory boards of Centenara Labs (formerly Rejuveron Life Sciences), Hevolution, and Institut Servier. G.K. is the inventor of patents covering therapeutic targeting of ACBP/DBI, aging, cancer, cystic fibrosis and metabolic disorders. G.K. has been holding research contracts with Daiichi Sankyo, Kaleido, Lytix Pharma, PharmaMar, Osasuna Therapeutics, Samsara Therapeutics, Sanofi, Sutro, Tollys, and Vascage. G.K.'s wife, Laurence Zitvogel, has held research contracts with Glaxo Smyth Kline, Incyte, Lytix, Kaleido, Innovate Pharma, Daiichi Sankyo, Pilege, Merus, Transgene, 9 m, Tusk, and Roche,

was on the Board of Directors of Transgene, is a cofounder of everImmune, and holds patents covering the treatment of cancer and the therapeutic manipulation of the microbiota. G.K.'s brother, Romano Kroemer, was an employee of Sanofi and now consults for Boehringer-Ingelheim. All other authors declare that they have no conflicts of interest. This study was funded by the TUM School of Medicine, the Deutsche Forschungsgemeinschaft (DFG, German Research Foundation, project ID 39535750 – SFB 1371 to J.C.F. and K.S.), the Else Kröner-Fresenius-Stiftung (2019\_A149 and 2022\_EKMS\_26 to J.C.F.), the German Cancer Aid (70113964 to J.C.F.). J.C.F. was supported by the Else Kröner-Forschungskolleg of the Technical University of Munich. V.R.T. and A.Z. were supported by Promotionssprogramm Translationale Medizin (V.R.T: Else Kröner Graduate School for Medical Students) of the Technical University of Munich. The funders had no role in the design of the study; in the writing of the manuscript, or in the decision to publish the results.

Data Sharing Statement: All data relevant to the study are included in the article. This study did not generate new unique reagents, biological material, or codes. Any additional information is available from the corresponding author on reasonable request.

Acknowledgments—We thank Olga Seelbach and the comparative experimental pathology team, as well as Hannah Felchle, for their technical assistance.

<sup>1</sup>These authors contributed equally.

Supplementary material associated with this article can be found in the online version at [doi:10.1016/j.ijrobp.2025.04.008](https://doi.org/10.1016/j.ijrobp.2025.04.008).

**Purpose:** Combining immune checkpoint inhibitors (ICIs) with radiation therapy (RT) has led to significant advancements in cancer treatment. However, evidence from clinical and experimental studies suggests that this combination may increase hematopoietic and lymphatic toxicity. This study aims to investigate the effects of the concurrent application of ICIs (anti-PD-1 and anti-CTLA-4) on radiation-induced hematopoietic and lymphatic injuries under standardized and controlled experimental conditions.

**Methods and Materials:** We used various experimental models in C57BL/6 and BALB/c mice to evaluate the impact of ICIs combined with RT on the hematopoietic system. These models involved different RT doses, regimens, and target sites in both healthy and tumor-bearing mice.

**Results:** Our findings showed that the concurrent use of ICIs did not meaningfully affect post-RT pancytopenia kinetics or the regeneration of specific blood cell lineages over time. Consistently, combining RT with ICIs did not significantly enhance DNA damage in immune cells within the bloodstream. This outcome was comparable across different RT doses, regimens, and target sites and was reproducible in both tumor-bearing and nontumor-bearing mice. Additionally, there were no significant increases in late side effects, including reductions in bone marrow cell counts or megakaryocyte numbers, after combined radioimmunotherapy.

**Conclusions:** These findings suggest that combining ICIs with RT does not exacerbate hematological toxicity. This information is valuable for interpreting adverse events in clinical trials involving radioimmunotherapy and for predicting potential hematological side effects in cancer patients receiving these treatments. © 2025 The Author(s). Published by Elsevier Inc. This is an open access article under the CC BY license (<http://creativecommons.org/licenses/by/4.0/>)

## Introduction

The discovery in the 19th century that some of those cancer patients who simultaneously suffered from infections experienced a regression of their malignancy marked the beginning of immunotherapy.<sup>1,2</sup> More than a century later, the development of the immune checkpoint inhibitors (ICIs) anti-CTLA-4 and anti-PD1/PD-L1 revolutionized cancer therapy.<sup>3</sup> Since the day the first ICI has been approved, obvious questions regarding the therapeutic potential for combination with already established therapies such as radiation therapy (RT) have emerged.<sup>4</sup> With intense research efforts illuminating ever-more underlying mechanisms and pathways by which RT and ICI therapy is connected,<sup>5</sup> clinical breakthroughs soon followed, e.g. for patients suffering from diseases such as advanced-stage lung and esophageal cancer.<sup>6-8</sup>

However, although hundreds of clinical studies combining RT with ICIs were initiated, many of them ended disappointingly, without proving beneficial results.<sup>9,10</sup> Moreover, even when successful, the flip side of strong positive effects is a correspondingly high potential for negative effects when combining 2 therapeutic approaches that boast a number of adverse events (AEs) during treatment even on their own. This potential risk of developing enhanced side effects following combined radioimmunotherapy remains incompletely understood—a gap in knowledge that negatively affects treatment planning and informed decision-making in daily patient care.<sup>11,12</sup>

RT induces DNA damage and leads to the release of damage-associated molecular patterns (e.g., ATP) and inflammatory cytokines (e.g., type I interferon). This process, collectively referred to as immunogenic cell death, on the one hand, drives the induction of an antitumor immune response but also fuels local inflammation in normal tissue, leading to local side effects and wide-ranging symptoms beyond the site of irradiation.<sup>5,13</sup> Meanwhile, ICIs have their

own set of AEs, that, due to their nature, are mostly so-called immune-related AEs (irAEs), whose toxicity can manifest on the tissue of almost every organ, both in the short-term as well as in the long-term.<sup>14,15</sup>

Nonetheless, scientific work available for evaluating side effects after the combination of RT and ICI was as recently as 4 years ago described as “largely unexplored,”<sup>16</sup> and expert consensus guidelines for combination therapy are still based on limited evidence.<sup>11,17</sup> Even comprehensive database analyses like the one done by Anscher et al<sup>18</sup>—who assessed more than 25,000 patients to investigate the rate of serious AEs for patients receiving RT and ICI—have to label their results as “only exploratory” when describing, for example, thrombocytopenia as occurring more often for patients who received both RT and ICI, especially when within a shorter time-span of each other. With other side effects in Anscher et al’s<sup>18</sup> study being distributed more evenly, this is especially interesting because 3 recently published randomized phase III studies evaluating the combination of chemoradiation and PD-1/PD-L1 inhibition for locally advanced cervical cancer, small cell lung cancer, and squamous cell carcinoma of the head and neck found thrombocytopenia, anemia, and leukopenia as part of the increased toxicity experienced by patients receiving anti-PD-1.<sup>6,19,20</sup>

In general, the hematological system is known to suffer greatly from cancer, regardless of entity. Manifestations include anemia or thrombocytopenia, which have a considerable impact on the morbidity and mortality of patients.<sup>21</sup> Considering that RT is well known to cause such side effects<sup>22,23</sup> and hematological irAEs for ICIs, although rare, do present and can then present as extremely serious complications,<sup>14,24</sup> it seems prudent to expect the combination of RT with ICIs to possibly lead to a coaction of side effects with the potential for significant damage to the blood-producing system of any patient, posing serious questions regarding therapeutic safety.<sup>25</sup>

Here, we investigated the potential occurrence of AEs affecting the hematological system after combined radioimmunotherapy using murine models with standardized experimental conditions to overcome the limitations of clinical studies, which are often difficult to interpret due to various confounders and the absence of control groups for ethical reasons.

## Methods and Materials

### Study design

The overall objective of this study was to investigate hematological toxicity after RT in combination with ICIs. Mice were randomly assigned to different experimental groups after stratification according to age. No outliers were excluded or censored from any experiment to circumvent attrition bias. The histopathological assessment was blinded. For all studies, the number of animals is depicted in the figures, and the number of independent experiments is listed in the figure legends. Statistical tests are described in the figure legends of the individual experiments. The project did not include a power calculation due to its limited validity in animal studies of basic medical research.<sup>26</sup> This study does not contain any human material or patient data.

### Study approval

This study does not contain any human data. All animal experiments were approved by the local governmental authorities.

### Mice

Female C57BL/6J and BALB/c wild-type mice were acquired from Charles River Laboratories at 5 to 6 weeks old. Mice were given a minimum of a 1-week acclimatization period upon arrival and housed in individually ventilated cages (with a maximum of 8 animals per unit) with a 12-hour light-dark cycle environment and ad libitum access to food and water.

### Subcutaneous tumor model

All experiments were performed with certified CT26 colon carcinoma cells that were bought from ATCC (#CRL-2638) in 2022. Cells were cultured according to standard protocols with RPMI-1640 (#R8758, Sigma-Aldrich) supplemented with 10% fetal calf serum, 1% penicillin/streptomycin (10000 U/mL) and 1% L-glutamine (200 mM), and continuously tested to be free of mycoplasma. Cell culture prior to tumor induction was standardized and performed with cells with the same passage (P4) after thawing. Tumor models were conducted similarly to those previously described.<sup>27</sup>

Right and left upper hind legs (thighs) of BALB/c mice were shaved and a volume of 40  $\mu$ L phosphate-buffered saline (PBS) containing  $4.5 \times 10^5$  CT26 tumor cells was injected subcutaneously one day later. Tumor size was determined by measuring the length and width of the tumor with a caliper. Mice were euthanized when any of their tumors exceeded  $>300 \text{ mm}^2$  (length  $\times$  width) or presented with ulceration. For data analysis, tumor volume was calculated with the formula:  $\frac{1}{2} \times (\text{length} \times \text{width}^2)$ . On day 6 after tumor injection, mice were stratified based on tumor size and assigned to different groups, ensuring experimental groups with similar tumor sizes.

### Lung metastasis model

Tumor models were conducted similarly to those previously described.<sup>28</sup> The B16 murine melanoma cell line expressing the full-length chicken ovalbumin (henceforth referred to as B16.OVA) was cultured in complete Dulbecco's Modified Eagle Medium (DMEM) high glucose medium (#D6429, Sigma-Aldrich) and supplemented with 10% fetal calf serum and 1% penicillin/streptomycin (10000 U/mL). Tumor cells ( $1 \times 10^5$ ) were injected intravenously in a volume of 200  $\mu$ L PBS into the tail vein of C57BL/6 mice. Animals were monitored daily and were euthanized in case of significant weight loss, signs of respiratory insufficiency, or general indications of markedly reduced activity or pain. The remaining mice were euthanized and analyzed on day 26 after tumor injection. The weight of the entire lung, as well as the left and right lung, was measured. Lungs were photographed from the front and back after washing in PBS. Images were processed manually using Adobe Illustrator (Adobe Inc).

### Immunotherapy

Dual immune checkpoint inhibition with anti-PD-1 and anti-CTLA-4 is the standard of care for treating patients with certain malignancies (eg, malignant melanoma or colorectal cancer [CRC] expressing specific mutations) and is also well-established in experimental research.<sup>29-31</sup> Dose regimens were adapted from literature on mouse models investigating irAEs.<sup>32</sup> Nontumor-bearing animals that were part of designated cohorts received high dosages of combined therapy of ICIs, namely anti-CTLA-4 (clone 9H10, Leinco Technologies) and anti-PD-1 (clone RMP1-14, Leinco Technologies): 250  $\mu$ g each dissolved in phosphate-buffered saline (PBS; Sigma-Aldrich) were injected intraperitoneally in a 1-week time frame, 1 day before (D-1) and 6 days after (D6) RT. B16.OVA tumor-bearing mice received combination therapy with ICIs once per week starting on day 4 after tumor cell inoculation (total dose: 4  $\times$  250  $\mu$ g/mouse anti-PD1 plus 4  $\times$  250  $\mu$ g/mouse anti-CTLA-4). CT26 tumor-bearing mice received ICIs twice per week starting on day 6 after tumor cell inoculation (total dose: 4  $\times$  250  $\mu$ g/mouse anti-PD1 plus 4  $\times$  250  $\mu$ g/mouse anti-

–CTLA-4). Those cohorts not receiving ICIs were injected with pure PBS.

### RT of tumor-free mice

C57BL/6 animals receiving total body irradiation (TBI) were placed in a designated radiation cage and covered with a plastic plate on small studs approximately the height of a single mouse to ensure that animals would not stack on top of each other and each animal would receive the full dosage. The cage was then centered inside the CIX2 (Xstrahl) and RT was performed at a dose rate of 0.6 Gy/min (15 mA, 195 kV, copper filter). The single dose amounted to 5 Gy, whereas the animals that were part of the fractionated radiation regime cohort were irradiated on 4 consecutive days with 1.5 Gy. Animals that received targeted RT of the legs were anesthetized with an intraperitoneal injection of MMF, a mix of medetomidin (0.5 mg/kg), midazolam (5 mg/kg), and fentanyl (0.05 mg/kg), and fixed on a plastic base with 3 lead plates (each of 3 mm thickness, equaling 9 mm in total) shielding everything but the hindlegs before being irradiated in the exact same manner as the full-body cohort. Immediately after treatment, anesthesia was halted by subcutaneous injection of atipamezol (2.5 mg/kg), flumazenil (0.5 mg/kg), and naloxon (1.2 mg/kg) and mice were monitored on a heating pad until fully awake.

### RT of tumor-bearing animals

Anesthesia and RT of tumors were performed similarly to the targeted RT of the legs described in the section above. Subcutaneous tumors located on right and left thighs were irradiated on days 7, 8, and 9 after tumor cell inoculation with a total of  $3 \times 15$  Gy, while the rest of the body, including the lower hind legs and feet, were shielded (irradiation device: CIX2; target volume: right and left tights of hind limbs; dose rate 1.33 Gy/min; beam time: 11 minutes 15 seconds per 15 Gy). Mice with lung metastases received RT with  $5 \times 9$  Gy to the right lung (days 4–8 after intravenous tumor cell inoculation), while the rest of the body was shielded (irradiation device: Gulmay [Xstrahl]; target volume: right lung; dose rate 0.95 Gy/min beam time 9 minutes 27 seconds per 9 Gy).

### Blood count

Blood was collected in EDTA tubes at different time points after RT and blood cells were counted automatically at the Institute of Clinical Chemistry and Pathobiochemistry of the Technical University of Munich using modules of the Sysmex XN series (Sysmex Europe GmbH). Endpoints included red blood cells, hemoglobin, thrombocytes, and

white blood cells, with differentiation into neutrophils and lymphocytes, if indicated in the figure.

### Flow cytometry

Single-cell suspensions were stained with a viability dye (Live-Dead Cyan, Invitrogen, #65-0866-18), FC receptor was blocked with an anti-CD16/32 antibody (Biologend, clone S17011E, #156604), and antibodies (CD45-APC - Cy7, Biolegend #103116; CD45 - FITC, Biolegend #103108; CD335 (NKp46) – PE, Biolegend #137604; NK1.1 – PB, Biolegend #108722; CD45R/B220 – APC, Biolegend #103212) followed by fixation/permeabilization (Foxp3/Transcription Factor Staining Buffer Set, eBioscience #00-5523-00) and intracellular staining (CD8 – PerCP-Cy5.5, Biolegend #100734; CD4 – Pe-Cy7, Biolegend #100434; gH2AX – PE, Biolegend #613412; gH2AX – APC/Fire750, Biolegend #613421; FoxP3 – PB, Biolegend #126410). Cell numbers were assessed using counting beads (CountBright Absolute Counting Beads). Flow cytometry was performed on a CytoFLEX (Beckman Coulter), and data were analyzed with FlowJo 10 software (BD).

### Bone marrow cell count

On day 150 and after having been bled, animals were euthanized and both tibiae and femurs were dissected and cleaned. One femur and both tibiae of each mouse were cut open at the knee-side so as to expose the bone marrow (BM) and, with that side facing down, put into 0.5 mL Eppendorf that had previously been punctured at the bottom with a 19 gauge needle. Bones in tubes were then transferred into a 1.5 mL Eppendorf tube containing 100  $\mu$ L of the completed medium, consisting of RPMI-1640-medium plus 10% fetal calf serum plus 1% penicillin/streptomycin plus 0.1%  $\beta$ -mercaptoethanol, and centrifuged for 1 minute at 2500g at room temperature. The flushed-out BM in the 1.5 mL tubes was resuspended with 1 mL of medium 10 times before straining the cell suspension through a 70  $\mu$ m cell strainer into a 15 mL Falcon tube. Having rinsed the 1.5 mL tubes with 1 mL of medium, the 15 mL Falcon tubes were placed in a centrifuge for 5 minutes at 300g at room temperature before removing the supernatant and resuspending the cells in 1 mL of red blood cell Lysis (G-DEXIIb RBC Lysis Buffer, iNtRON). After 5 minutes, the lysis was stopped by adding a total of 5 mL of medium. Centrifuging for 5 minutes at 300g, removing supernatant, and resuspending cells in 5 mL of medium was the last step before 2 separate counts of each sample were performed.

### Histopathological analysis

After dissection, the right femur of every animal was cleaned and put into neutral buffered 10% formalin solution (Sigma-Aldrich) for 48 hours before being transferred into a

decalcifying agent (OSTEOSOFT, Sigma-Aldrich) for another 2 days to soften the tissue. The bones were then put back into formalin and handed over to the Institute of Pathology of the TU Munich to be stained using a standard hematoxylin and eosin staining procedure, placed in paraffin wax, and cut lengthwise. Images of the resulting slides were captured digitally and then analyzed using QuPath by first defining a maximum of 10 scorable fields with a size of  $400 \times 400 \mu\text{m}$ , equaling a square of  $0.16 \text{ mm}^2$ , for each slide. Because megakaryocytes are easily distinguishable from other cells commonly present in BM due to their greater size and distinct morphology, they could then be counted easily by hand, as has been described previously.<sup>33</sup> The researcher performing the count did not know which sample belonged to which cohort.

## Statistics

All data are presented as the mean with standard deviation. The number of pooled experiments are indicated in figure legends. Statistical analyses were performed using GraphPad Prism version 9.3.0 (GraphPad Prism Software). Differences between means of experimental groups were analyzed by using ordinary 1-way ANOVA for multiple comparisons (Dunnett's correction) or unpaired 2-tailed *t* test if only 2 groups were compared. The types of tests are indicated in the figure legends. *P* values are mentioned in the figures.

## Results

First, to exclusively study the possible exacerbation of hematological toxicity after irradiation when combined with ICIs, we applied conventional experimental models of irradiation-induced lymphatic and hematopoietic injury.<sup>34</sup> We found that TBI with a single dose of 5 Gy resulted in measurable toxicity for otherwise healthy and untreated C57BL/6 mice: white blood cell count was lowest on day 7 and steadily recovered to physiological levels within 2 months (Fig. 1A). Red blood cell count was close to normal levels on day 7 but dipped on day 14 before returning to previous levels on day 28 (Fig. 1B). Platelet count had its nadir on day 14 before improving to prior levels (Fig. 1C), and hemoglobin showed a similar progression over time like red blood cell count (Fig. 1D). Comparing these kinetics to those of mice receiving RT combined with ICIs (anti-CTLA4 and anti-PD-1), the trends were virtually the same (Fig. 1A-D). Mice treated only with ICIs showed practically no difference in measurements whatsoever compared to control mice (Fig. 1A-D).

Because different fractionation regimens have a significant impact on immuno-oncology outcomes in terms of tumor control as well as toxicity to normal tissue<sup>5,13</sup> and fractionated RT is a widely used part of daily patient care, we changed the RT regimen from one single dose to a fractionated therapy approach ( $4 \times 1.5 \text{ Gy TBI}$ ). For these

conditions, white blood cell count was measured as its lowest on day 7, whereas platelet count, red blood cell count, and hemoglobin were the lowest on day 14, with full recovery achieved for all parameters within 2 months (Fig. 1E-H). As was true for the single-dose setting, the fractionated setting also did not show any discernible difference for any of the values investigated by us between mice receiving radiation only and mice receiving additional ICIs (Fig. 1E-H).

Next, we turned our attention to chronic injury and late side effects and performed a multilevel analysis on day 150 after irradiation. When assessing the complete blood count, the white blood cell count was lowest for the group having received a single dose of 5 Gy, but even here, as for all other groups, levels were within physiological boundaries (Fig. 2A). Because lymphocyte and neutrophil counts are of great clinical relevance,<sup>5,35</sup> we also compared these subsets of white blood cells and could not find any significant differences in levels for mice that did or did not receive ICI additionally to single dose RT (Fig. 2B, C). Consistently, we did not observe significantly reduced neutrophil counts after fractionated RT compared to fractionated RT combined with ICIs (Fig. 2C). However, there were significantly reduced lymphocyte numbers in this setting (Fig. 2B). Despite this, total lymphocyte numbers were similar to those in untreated mice, indicating no increased toxicity after combined radioimmunotherapy (Fig. 2B). Similar uniform appearance for all groups held true for red blood cell count, platelet count and hemoglobin measurements (Fig. 2D-F).

Next, we explored potential damage to the locus of blood cell production and maturation by assessing the number of viable BM cells after RT. To this end, we could not record any significant dissimilarity for any of the previously described groups: for both settings of RT ( $1 \times 5 \text{ Gy TBI}$  vs  $4 \times 1.5 \text{ Gy TBI}$ ), the added strain of ICI therapy did not result in significantly changed numbers of BM cells in the femur or the tibiae, and, what is more, did not differ from the figure recorded for control mice or those receiving only ICIs (Fig. 2G, H). Additionally, we compared the numbers of megakaryocytes in the BM between the cohorts as platelets are specifically considered to be affected by combination therapy of RT and ICIs.<sup>18</sup> However, adding ICIs to both settings of single-dose and fractionated RT did not have any significant impact on the number of megakaryocytes counted (Fig. 2I, J).

Because experimental models applying TBI do not only induce hematopoietic and lymphatic injury but also can lead to systemic inflammation, e.g., via intestinal epithelial tissue damage and subsequent barrier dysfunction, which in turn can affect hematopoiesis and the BM,<sup>13,36</sup> as well as having a pronounced effect on ICI therapy,<sup>37</sup> we performed targeted irradiation of the lower extremities of the animals, representing a significant fraction of the BM, while sparing the rest of their body, in order to zero in on the relevant physiological niche. Blood work done on day 14 and day 60 did not reveal significant differences regarding red blood cells, thrombocytes, and hemoglobin when comparing

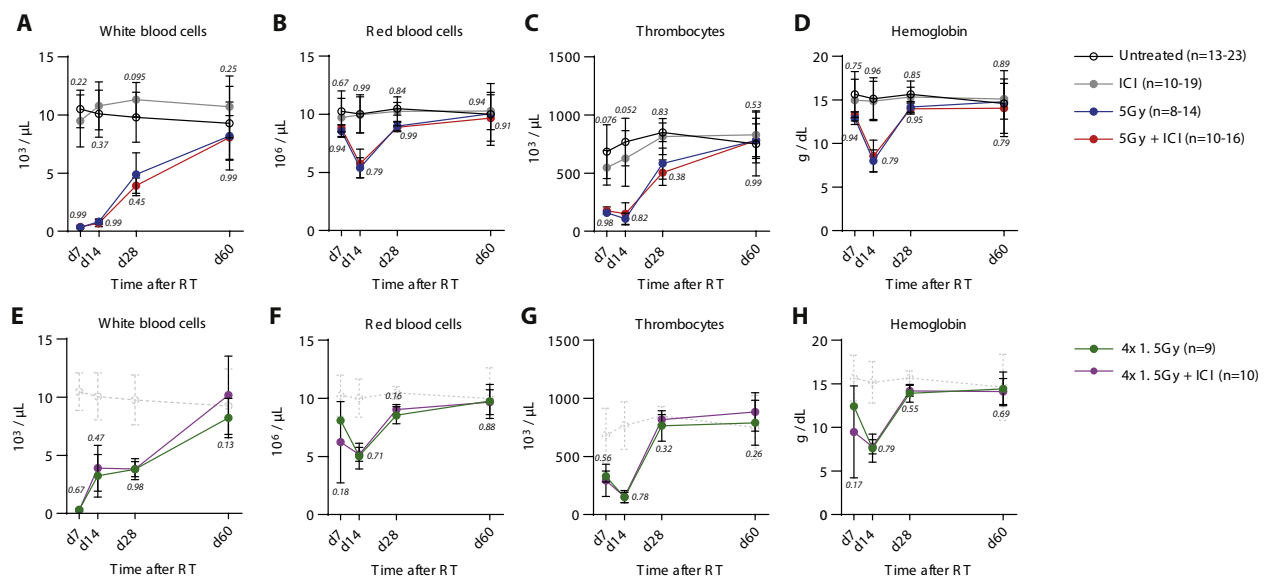


**Fig. 1.** Concomitant immune checkpoint inhibition does not significantly aggravate short-term injury to the hematological system after total body irradiation (TBI). (A-D) C57BL/6 mice received a single dose of radiation therapy (RT) (5 Gy TBI) ± anti-PD-1 and anti-CTLA-4 (2 injections, weekly, starting 1 day prior to RT). Blood of mice was drawn via buccal vein puncturing on indicated time points after RT and blood cell populations and hemoglobin concentration were assessed with a blood analyzer. The kinetics of the (A) white blood cell population, (B) red blood cell population (erythrocytes), (C) thrombocyte population (platelets), and (D) hemoglobin are presented. Pooled data are from 6 independent experiments. The data were analyzed using 1-way ANOVA and are presented as mean  $\pm$  SD. (E-H) C57BL/6 mice received a fractionated RT (4  $\times$  1.5 Gy TBI) ± anti-PD-1 and anti-CTLA-4. (E) The kinetics of the white blood cell population, (F) red blood cell population, (G) thrombocyte population and (H) hemoglobin are presented. The dotted gray line represents untreated mice (data also shown in the upper panel; n = 13-23 mice). Pooled data are from 2 independent experiments. The data were analyzed using unpaired 2-tailed t tests and are presented as mean  $\pm$  SD. The number of mice (n) is shown in the figure. P values are presented in the figure. Abbreviations: ICI = immune checkpoint inhibitor.

groups having been treated only with RT or having received additional therapy with ICIs (Fig. 3A-D). Finally, we analyzed late AEs in this specific setting; where data for chronic injury on day 150 once again did not show significant differences when comparing white blood cell, lymphocyte, neutrophil, red blood cell, thrombocyte count, or hemoglobin levels between the 2 cohorts of mice that received ICIs along with RT and those that did not (Fig. 3E-J). Accordingly, we also did not note any significant difference in the number of cells counted in the femur and tibiae (Fig. 3K, L) and the number of megakaryocytes counted in the BM (Fig. 3M, N).

Next, we aimed to validate our findings in tumor-bearing mice treated with clinically relevant RT regimens. Metastatic melanoma is commonly managed with ICIs, including dual inhibition with anti-PD-1 and anti-CTLA-4.<sup>30</sup> Moreover, RT of selected metastases (eg, in scenarios of oligoprogressive disease) is common clinical practice.<sup>11,30,38,39</sup> To mimic this scenario, we utilized a mouse model of pulmonary metastasized melanoma. As expected, treatment of tumor-bearing lungs with 5  $\times$  9 Gy RT significantly reduced tumor load, both with and without additional ICIs. In contrast, ICIs alone were less effective in reducing tumor progression in this aggressive model (Fig. E1A-C). Combining RT with ICIs resulted in significantly increased red blood cell count concentrations after combination therapy (Fig. 4A, B).

Enhanced anemia in this B16 tumor model has been well-described in previous studies; thus, we conclude that reducing the tumor load counterbalances this effect.<sup>40,41</sup> Moreover, we did not observe significant changes in thrombocytes and white blood cell concentrations after combination therapy (Fig. 4C-F). More specific analyses failed to reveal any significant changes in CD4<sup>+</sup> T helper cells, CD8<sup>+</sup> cytotoxic T cells, B cells, or natural killer cells between irradiated mice and those receiving combined radioimmunotherapy (Fig. 4G-J; Fig. E1D). Thus, we hypothesize that ICIs did not result in enhanced killing of circulating immune cells during RT. Accordingly, we did not observe any significantly increased signs of DNA damage (phosphorylated  $\gamma$ H2AX) at the end of RT when combined with ICIs (Fig. 4K-O; Fig. E1E).

Lastly, we aimed to generalize our results by investigating a disparate tumor entity growing on a different mouse strain to preclude our observations from being restricted to a specific genetic background, tumor entity, or anatomical treatment site. Patients with metastatic CRC significantly benefit from dual ICI therapy if they harbor specific mutations<sup>31</sup> and clinical studies are investigating the potential of combining ICIs with additional RT for tumor lesions in metastatic CRC.<sup>42</sup> As one would therefore expect, local therapy of subcutaneously implanted CRC tumors (right and left

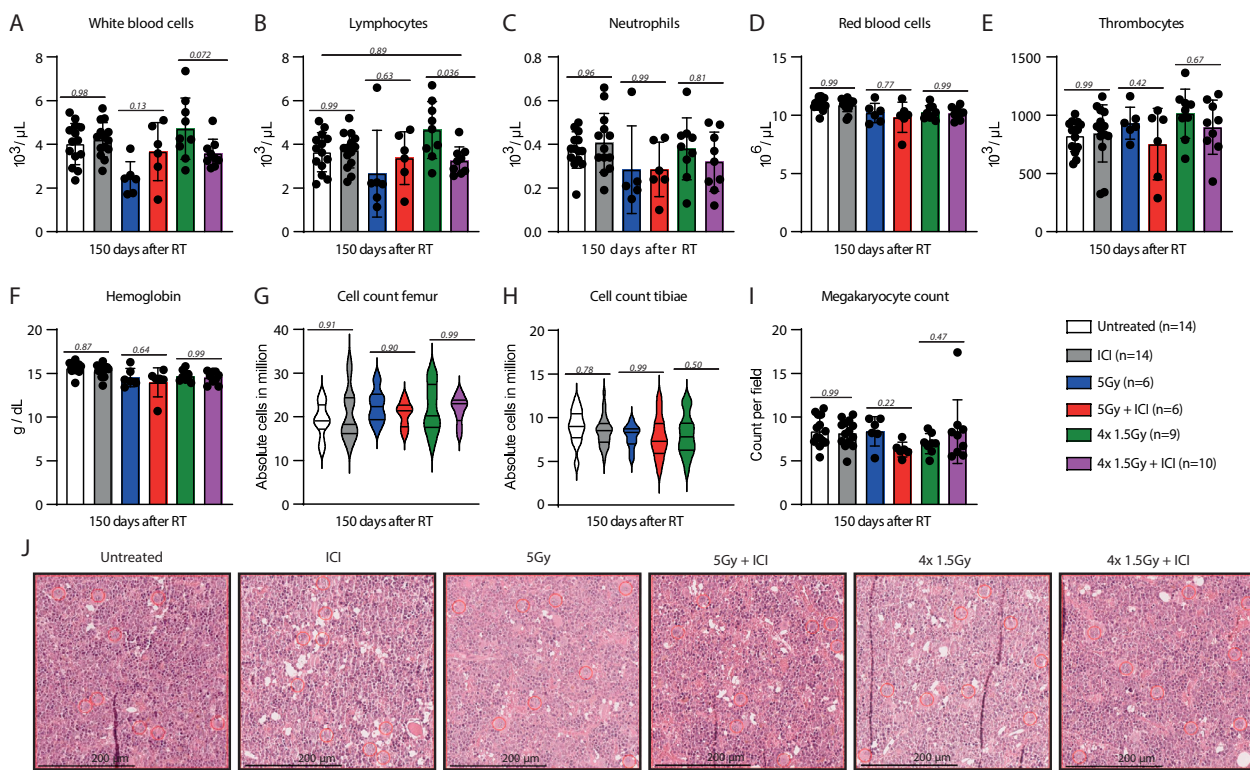


**Fig. 2.** Concomitant immune checkpoint inhibition does not significantly aggravate long-term injury to the hematological system after total body irradiation (TBI). (A-F) C57BL/6 mice received single-dose (5 Gy TBI) or fractionated radiation therapy (RT) ( $4 \times 1.5$  Gy TBI)  $\pm$  anti-PD-1 and anti-CTLA-4 (2 injections, weekly, starting 1 day prior to RT). Blood of mice was drawn via buccal vein puncturing on day 150 after RT and assessed with a blood analyzer. The levels of (A) white blood cell population, (B) lymphocytes, (C) neutrophils, (D) red blood cell population, (E) thrombocytes, (F) and hemoglobin were assessed with a blood analyzer. Each dot represents data from one animal. (G-J) The bones of the mice were analyzed on day 150 after irradiation. (G) Absolute number of bone marrow cells of the right femur bones and (H) both tibia bones of the mice. Data are shown as a violin plot, with a line showing the median. (I) The left femur bones were processed for histopathological analysis and  $200 \times 200 \mu\text{m}$  sized fields of view in hematoxylin and eosin-stained longitudinal sections of the bone marrow were evaluated in regard to number of megakaryocytes (MGKC). Data are shown as mean  $\pm$  SD number of MGKC per field. On average 10 fields were counted per mouse. (J) Representative images of untreated mice and mice treated with the immune checkpoint inhibitor (ICI), mice receiving RT, mice receiving RT plus ICI, mice receiving fractionated RT, and mice receiving fractionated RT plus ICI, with MGKC marked by red circles. The data were analyzed using 1-way ANOVA and are presented as mean  $\pm$  SD. Pooled data from 4 independent experiments. The number of mice (n) is shown in the figure. P values are presented in the figure.

hind legs) with  $3 \times 15$  Gy significantly reduced tumor growth, and this effect was improved by the addition of ICIs (Fig. E2A). Combining RT with ICIs failed to significantly impact most blood cell lineages and hemoglobin concentrations, but significantly reduced thrombocytes at early time points (1 week) (Fig. 5A-F). Similarly to the lung metastasis model, ICI did not exacerbate the effects of RT on the frequencies of different immune cell subpopulations (Fig. 5G-J) or the intensity of DNA damage responses after RT (Fig. 5K-O; Fig. E2B).

## Discussion

In our study, we examined BM and peripheral blood cell populations after radioimmunotherapy, which, to the best

of our knowledge, is the first experimental investigation addressing this matter. Our results did not reveal any pronounced differences in acute or late side effects following combination therapy, regardless of the fractionation regimen or the irradiation site, in either healthy or tumor-bearing mice. These data from standardized and controlled experiments are valuable, considering that large databank analyses and recent randomized phase III studies have suggested a potential increase in hematological toxicity (e.g., thrombocytopenia),<sup>6,18-20</sup> and experimental studies have found that ICIs combined with RT can result in the enhanced killing of immune cells.<sup>43,44</sup>

When considering how RT and ICI influence each other, it is already known from previous studies that RT can increase tumor immunogenicity, prime antitumor T cells, upregulate surface molecules for better immune recognition,

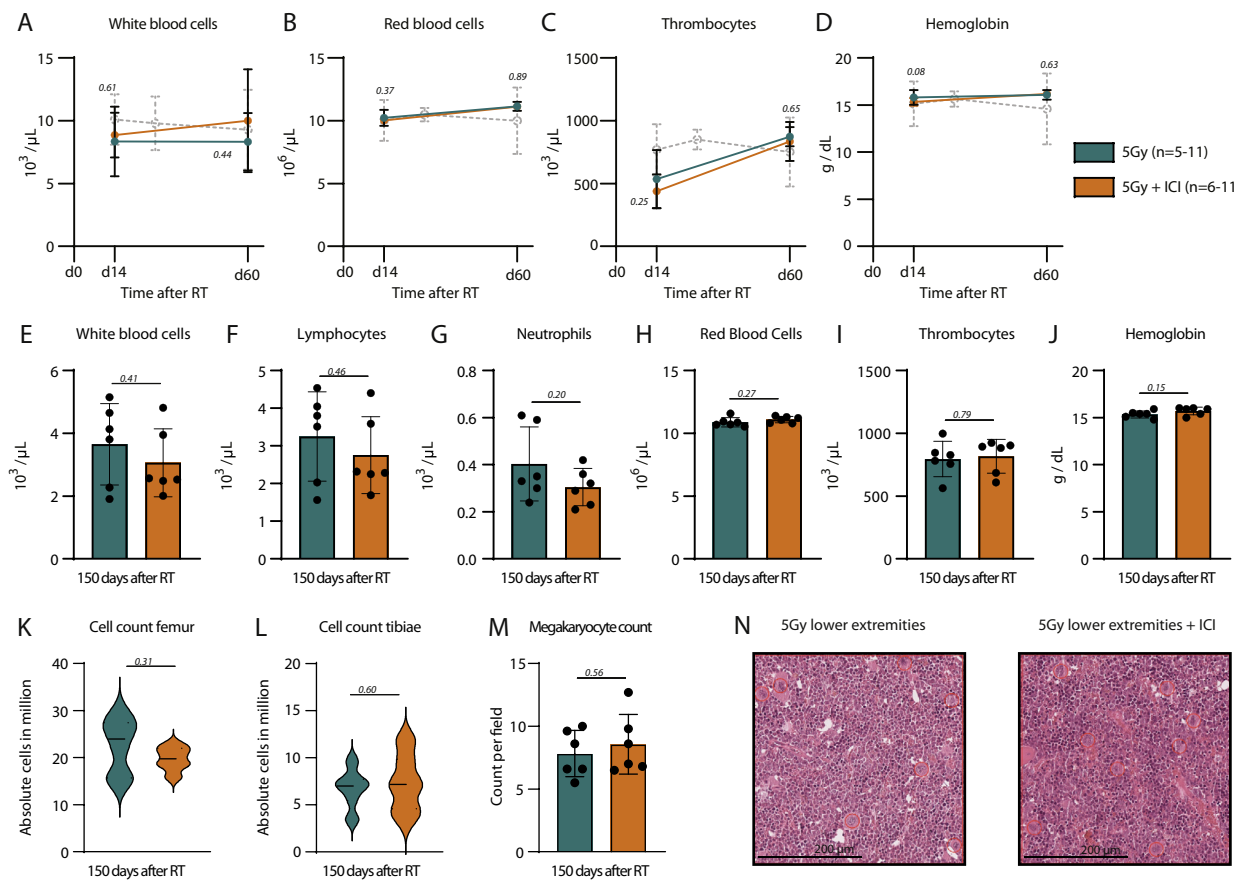


**Fig. 3.** Concomitant immune checkpoint inhibition in combination with targeted irradiation of the legs does not appreciably enhance short- or long-term hematological toxicity. (A-N) C57BL/6 mice received a single dose of radiation therapy (RT) (5 Gy) to the lower extremities only  $\pm$  anti-PD-1 and anti-CTLA-4 (2 injections, weekly, starting 1 day prior to RT). Levels of the (A) white blood cell population, (B) red blood cell population, (C) thrombocytes, and (D) hemoglobin on day 14 and 2 months after irradiation were assessed with a blood analyzer. The dotted gray line represents untreated mice (data also shown in Fig. 1). Levels of (E) white blood cell population, (F) lymphocytes, (G) neutrophils, (H) red blood cells, (I) thrombocytes, (J) and hemoglobin on day 150 after RT were assessed with a blood analyzer. Pooled data are from 3 independent experiments. (K) Absolute number of bone marrow cells of the right femur bones and (L) both tibia bones of the mice. Data are shown as a violin plot, with the line showing the median. (M) The left femur bones were processed for histopathological analysis and  $200 \times 200 \mu\text{m}$  sized fields of view in hematoxylin and eosin-stained longitudinal sections of the bone marrow were evaluated in regard to number of megakaryocytes (MGKC). Number of MGKC per field of view. On average 10 fields were counted per mouse. (N) Representative images of untreated mice and mice treated with the immune checkpoint inhibitor (ICI), mice receiving RT, mice receiving RT plus ICI, mice receiving fractionated RT, and mice receiving fractionated RT plus ICI, with MGKC marked by red circles. Pooled data are from 2 independent experiments. The data were analyzed using unpaired 2-tailed *t* tests and are presented as mean  $\pm$  SD. The number of mice (n) is shown in the figure. *P* values are presented in the figure.

and improve ICI therapy through a host of further mechanisms.<sup>5,45</sup> Our examinations of hematological markers add to the existing literature, where reports on the increased toxicity of combined radioimmunotherapy versus monotherapy have often been mixed and unclear. Reports of definitively increased toxicity of additional immune therapy under RT regimes, i.e., for the heart,<sup>46,47</sup> are as common as reports of failure to confirm observations in controlled and standardized contexts, as was the case for skin injury.<sup>7,48</sup> The fact that even the previously mentioned study by Anscher et al.,<sup>18</sup> screening multiple thousand patients,

revealed major limitations (like the inability to perform investigations of the RT site, dose, and fractionation, as well as statistical analyses) for their findings of enhanced side effects like reactions of the pulmonary system, the endocrine system or even more general symptoms like fatigue, stresses the urgent need for standardized experimental investigations into these inquiries.

Concerning hematopoietic toxicity, our data are consistent with a randomized phase III study published by Lee et al.,<sup>10</sup> investigating whether the addition of the a-PD-L1 drug avelumab to standard-of-care chemoradiation therapy would

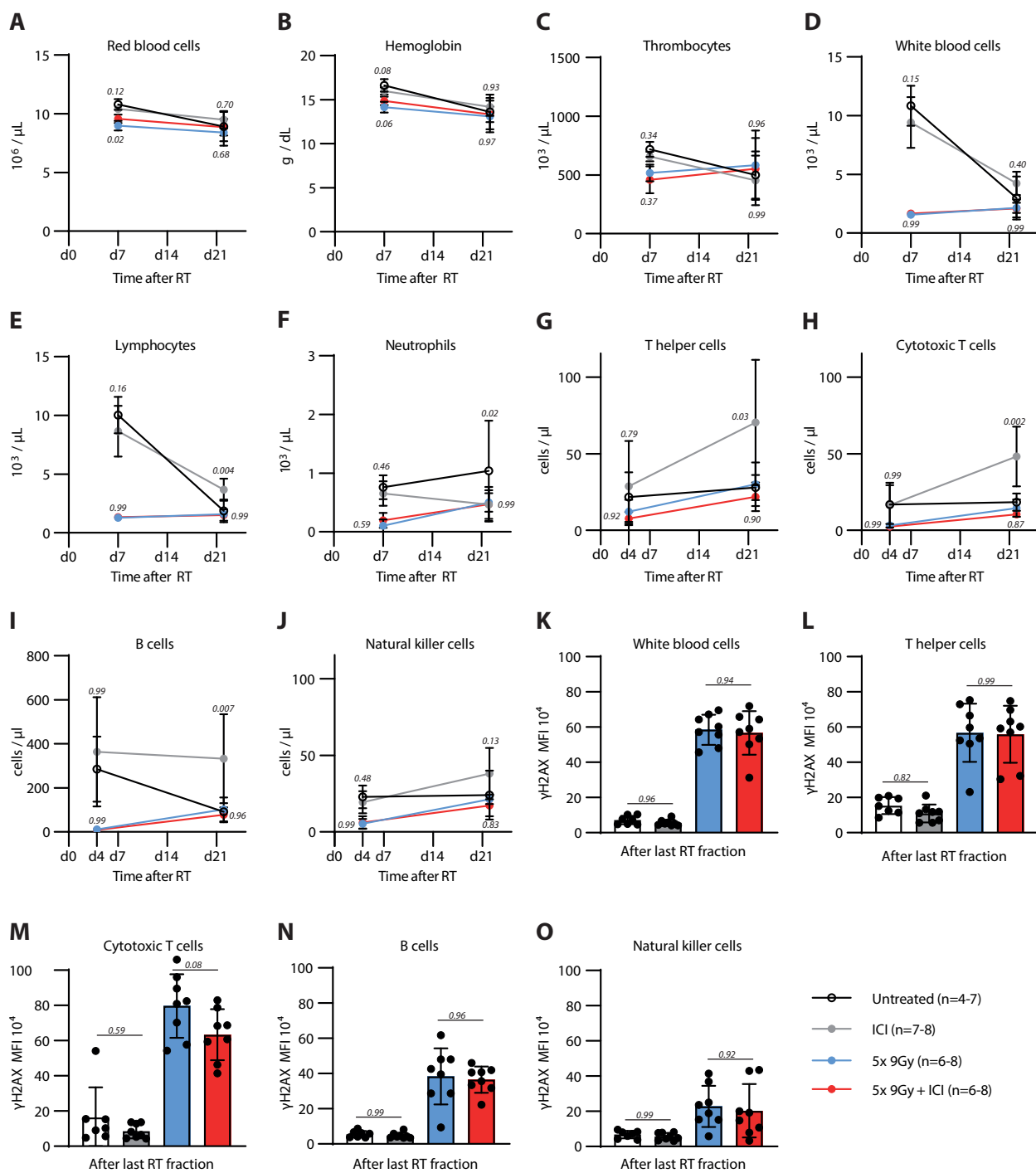


**Fig. 4.** Combined radioimmunotherapy of the lungs with metastatic melanoma does not significantly enhance hematological toxicity or DNA damage responses in circulating immune cells. (A-O) C57BL/6 mice received the B16 murine melanoma cell line expressing the full-length chicken ovalbumin melanoma cells intravenously 4 days before the start of therapy: Fractionated radiation therapy (RT) ( $5 \times 9$  Gy) to the right thorax  $\pm$  anti-PD-1 and anti-CTLA-4 (4 injections, weekly, starting in parallel with RT). Levels of the (A) erythrocytes, (B) hemoglobin, (C) thrombocytes, (D) white blood cell population, (E) lymphocytes, and (F) neutrophils on days 7 and 22 after onset of RT. Blood levels of (G) CD4 $^+$  cells T helper cells, (H) CD8 $^+$  cytotoxic T cells, (I) B220 $^+$  B cells, and (J) NK1.1 $^+$  natural killer cells were analyzed by flow cytometry in combination with counting beads, directly after completing RT and on day 22 after onset of RT. (K-O) The intensity of the phosphorylated  $\gamma$ H2AX signal of respective immune cell subpopulations was assessed by flow cytometry directly after completing the last fraction of RT and the mean fluorescence intensity (MFI) is presented. The figure shows data from 1 experiment analyzed using 1-way ANOVA. Data are presented as mean  $\pm$  SD. The number of mice (n) is shown in the figure. P values are presented in the figure. Abbreviations: ICI = immune checkpoint inhibitor.

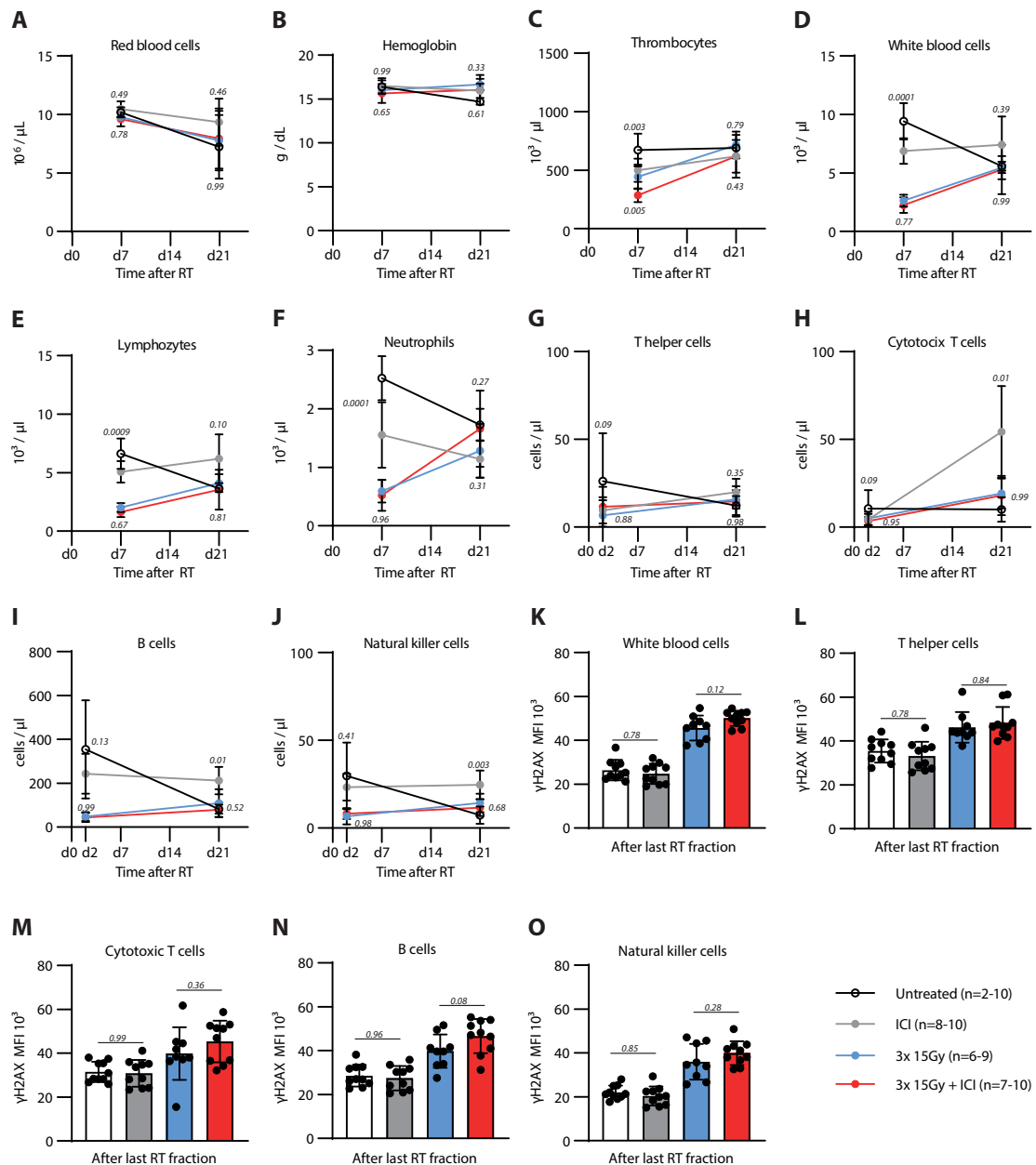


**Fig. 5.** Combined radioimmunotherapy of CRC metastases in the upper limbs does not significantly enhance hematological toxicity, except for acute platelet reduction. (A-O) BALB/c mice received subcutaneous CT26 tumor cell injections into both upper hind legs 1 week before therapy: Fractionated radiation therapy (RT) (3 × 15 Gy) to both upper hind legs ± anti-PD-1 and anti-CTLA-4 (4 injections, twice per week, starting 1 day prior to RT). Levels of the (A) red blood cells, (B) hemoglobin, (C) thrombocytes, (D) white blood cell population, (E) lymphocytes, and (F) neutrophils on days 7 and 21 after onset of RT. Blood levels of (G) CD4<sup>+</sup> cells T helper cells, (H) CD8<sup>+</sup> cytotoxic T cells, (I) B220<sup>+</sup> B cells, and (J) NKp46<sup>+</sup> natural killer cells were analyzed by flow cytometry in combination with counting beads, directly after completing RT and on day 21 after onset of RT. (K-O) The intensity of the phosphorylated γH2AX signal of respective immune cell subpopulations was assessed by flow cytometry directly after completing the last fraction of RT and the mean fluorescence intensity (MFI) is presented. Pooled data are from 2 independent experiments. The data were analyzed using 1-way ANOVA and are presented as mean ± SD. The number of mice (n) is shown in the figure. P values are presented in the figure. Abbreviations: ICI = immune checkpoint inhibitor.

improve outcomes for head and neck cancer patients, which revealed comparable rates of neutropenia and anemia, similar to the findings by Kelly et al<sup>8</sup> for esophageal cancer or Antonia et al<sup>7</sup> for Non-small-cell lung cancer (NSCLC). On the

flip side however, Lorusso et al<sup>19</sup> showed more hematological toxicity (e.g., including thrombocytopenia, anemia, and leukopenia) after combined radio-chemo-immunotherapy for the treatment of cervical cancer, a finding that is supported

by Machiels et al<sup>20</sup> for the treatment of locally advanced squamous cell carcinoma of the head and neck with pembrolizumab and chemoradiation therapy. Similarly, Cheng et al<sup>6</sup> found enhanced anemia in patients treated with durvalumab after chemoradiation therapy in limited-stage small cell lung cancer. Notably, the effect sizes of the observed phenomena are rather small for most of the analyzed endpoints, with the proviso, however, that irradiation sites were clearly defined, and the majority of the patients' BM thus presumably remained unaffected.

Because our study discovered a reduction in thrombocytes at early time points after combined radioimmunotherapy of peripheral sites but not after therapy of lung metastases, new questions arise. Additional studies are needed to understand the driving factors behind this phenomenon, such as the relative impact of anti-PD-1 versus anti-CTLA-4 or the pathophysiological relevance of the irradiation site. Moreover, the cancer entity itself might also be a confounding factor, as certain tumors (e.g., B16 melanoma) can induce dysregulated hematopoiesis, promoting anemia and thrombocytopenia.<sup>49</sup>

Nonetheless, multiple studies stress that AEs affecting the hematological system account for serious clinical complications during the treatment of patients with ICI monotherapy: anemia, thrombocytopenia, neutropenia, and more have each been described by multiple authors.<sup>24,50-53</sup> Contrarily, we did not observe any significantly increased toxicity in mice treated with ICI monotherapy compared to untreated mice in our controlled experimental set-up.

Interestingly, several studies have found that ICI combined with RT can result in the local killing of proliferating immune cells (likely via enhanced DNA damage and subsequent apoptosis of activated cytotoxic T cells after anti-PD-1 treatment) and that simultaneous RT of the tumor and draining lymph nodes results in enhanced immune cell killing if combined with ICIs.<sup>43,44</sup> Considering that the hematopoietic stem cells in the BM and precursor cells are characterized by a high grade of proliferation, it appeared reasonable to speculate that combination therapy would have resulted in enhanced toxicity to proliferating cells. Although the analysis in our experimental set-up did not reveal a significant change in the BM, several authors have considered the negative impact that especially anti-PD-1 drugs can have on this compartment,<sup>50,54,55</sup> subsequently leading to (sometimes lethal) anemia.<sup>14,56</sup> Similarly, much lower dosages of radiation than what was used in our set-up have been described to cause significant damage and result in the so-called hematopoietic acute radiation syndrome,<sup>57</sup> whereas we did find a return to physiological levels, and in a much smaller time frame, too.

Our observation that the number of neutrophilic granulocytes or lymphocytes was not significantly reduced after combined radioimmunotherapy is of specific interest because reduced lymphocyte numbers, especially decreased T cell ratios, are generally associated with negative long-term outcomes in patients treated with ICIs, RT or combined radioimmunotherapy.<sup>5,58</sup> In contrast to the previously

mentioned experimental study that has found enhanced T cell killing and DNA damage after combination therapy,<sup>43</sup> we did not observe such phenomenon in circulating T cell subsets, B cells, and natural killer cells. However, because we primarily focused on broader subsets of circulating immune cells and did not investigate more specific immune cell subpopulations, including their functional state at the time of RT, further studies are needed to determine the specific conditions (e.g., activation status, cofactors) under which RT combined with ICIs leads to enhanced DNA damage and T cell killing, as previously described.<sup>43</sup>

Finally, a methodological finding of our study is the insight that a dosage of 5 Gy, when administered to the entire body, is sufficient to produce a measurable negative effect on various hematological cell populations in the bloodstream, but does not result in any serious AEs beyond the ones discussed before. This is in line with experiments conducted by Grande et al,<sup>34</sup> who were able to show a clear drop-off for the leukocyte population after irradiation with 4 Gy and further define a corridor for investigating irradiation effects on the hematological system that is still safe: where 8 Gy has in the past already resulted in a 90% mortality rate (even with added "support" for the hematopoietic system through administration of thrombopoietin),<sup>59</sup> none of our animals died due to RT. Our study expands these data by including additional fractionation regimens and targeted irradiation of the lower extremities, which will be helpful for future investigations of related inquiries.

Our study has limitations in that, although we performed a total of 5 different RT regimens, ranging from unfractuated TBI (eg, 1 × 5 Gy TBI) to fractionated high-dose RT of selected areas (eg, 3 × 15 Gy to the upper hind legs), resulting in strongly varying total doses, beam times, and irradiated volumes, our study did not formally assess precise estimations of, for example, irradiated blood volumes, which might influence outcomes in this setting. However, despite substantial differences in these radiobiological parameters, our data remain consistent across almost all endpoints—we therefore conclude that our findings can be considered largely independent of the said parameters. In addition, although we did not systematically investigate different ICI dosing regimens, which are known to influence the occurrence of irAEs,<sup>15</sup> our study employs high doses of dual ICI therapy (250 µg/mouse anti-PD-1 + 250 µg anti-CTLA-4, administered once or twice per week), exceeding the dosing used in well-established irAE models in other experimental settings.<sup>32</sup>

## Conclusions

In summary, we conclude that combined radioimmunotherapy does not exert any marked effects on the common blood cell lineages or the body's hematopoietic capacity in mice. With this approach becoming exponentially more important in the clinical setting, much of the underlying mechanisms still in the dark, and the existing body literature

providing inconsistent and conflicting findings, there remains an urgent need to study these effects more extensively and in different models: like many other experts, we believe that the precise causal relationships and underlying mechanisms remain incompletely understood. These findings highlight the need for further research to ensure the safe integration of RT and immunotherapy.<sup>5,9,45</sup>

## References

1. Tang J, Pearce L, O'Donnell-Tormey J, Hubbard-Lucey VM. Trends in the global immuno-oncology landscape. *Nat Rev Drug Discov* 2018;17:783-784 Published correction appears in *Nat Rev Drug Discov*. 2018;17:922.
2. Rui R, Zhou L, He S. Cancer immunotherapies: Advances and bottlenecks. *Front Immunol* 2023;14:1212476.
3. Korman AJ, Garrett-Thomson SC, Lonberg N. The foundations of immune checkpoint blockade and the ipilimumab approval decennial. *Nat Rev Drug Discov* 2022;21:509-528 Published correction appears in *Nat Rev Drug Discov*. 2022;21:163.
4. Ngwa W, Irabor OC, Schoenfeld JD, Hesser J, Demaria S, Formenti SC. Using immunotherapy to boost the abscopal effect. *Nat Rev Cancer* 2018;18:313-322.
5. Galluzzi L, Aryankalayil MJ, Coleman CN, Formenti SC. Emerging evidence for adapting radiotherapy to immunotherapy. *Nat Rev Clin Oncol* 2023;20:543-557.
6. Cheng Y, Spigel DR, Cho BC, et al. Durvalumab after chemoradiotherapy in limited-stage small-cell lung cancer. *N Engl J Med* 2024; 391:1313-1327.
7. Antonia SJ, Villegas A, Daniel D, et al. Durvalumab after chemoradiotherapy in stage III non-small-cell lung cancer. *N Engl J Med* 2017; 377:1919-1929.
8. Kelly RJ, Ajani JA, Kuzdzal J, et al. Adjuvant nivolumab in resected esophageal or gastroesophageal junction cancer. *N Engl J Med* 2021; 384:1191-1203.
9. Sharma P, Goswami S, Raychaudhuri D, et al. Immune checkpoint therapy-current perspectives and future directions. *Cell* 2023;186:1652-1669.
10. Lee NY, Ferris RL, Psyrri A, et al. Avelumab plus standard-of-care chemoradiotherapy versus chemoradiotherapy alone in patients with locally advanced squamous cell carcinoma of the head and neck: A randomised, double-blind, placebo-controlled, multicentre, phase 3 trial. *Lancet Oncol* 2021;22:450-462.
11. Kroeze SGC, Pavic M, Stellamans K, et al. Metastases-directed stereotactic body radiotherapy in combination with targeted therapy or immunotherapy: Systematic review and consensus recommendations by the EORTC-ESTRO OligoCare consortium. *Lancet Oncol* 2023;24: e121-e132.
12. Kraus KM, Fischer JC, Borm KJ, et al. Evaluation of practical experiences of German speaking radiation oncologists in combining radiation therapy with checkpoint blockade. *Sci Rep* 2021;11:7624.
13. De Ruysscher D, Niedermann G, Burnet NG, Siva S, Lee AWM, Hegi-Johnson F. Radiotherapy toxicity. *Nat Rev Dis Primers* 2019;5:13. Published correction appears in *Nat Rev Dis Primers*. 2019;5:15.
14. Postow MA, Sidlow R, Hellmann MD. Immune-related adverse events associated with immune checkpoint blockade. *N Engl J Med* 2018; 378:158-168.
15. Johnson DB, Nebhan CA, Moslehi JJ, Balko JM. Immune-checkpoint inhibitors: Long-term implications of toxicity. *Nat Rev Clin Oncol* 2022;19:254-267.
16. Mondini M, Levy A, Meziani L, Milliat F, Deutsch E. Radiotherapy-immunotherapy combinations — Perspectives and challenges. *Mol Oncol* 2020;14:1529-1537.
17. Meattini I, Becherini C, Caini S, et al. International multidisciplinary consensus on the integration of radiotherapy with new systemic treatments for breast cancer: European Society for Radiotherapy and Oncology (ESTRO)-endorsed recommendations. *Lancet Oncol* 2024; 25:e73-e83.
18. Anscher MS, Arora S, Weinstock C, et al. Association of radiation therapy with risk of adverse events in patients receiving immunotherapy: A pooled analysis of trials in the US food and drug administration database. *JAMA Oncol* 2022;8:232-240 Published correction appears in *JAMA Oncol*. 2022;8:306.
19. Lorusso D, Xiang Y, Hasegawa K, et al. Pembrolizumab or placebo with chemoradiotherapy followed by pembrolizumab or placebo for newly diagnosed, high-risk, locally advanced cervical cancer (ENGOT-cx11/GOG-3047/KEYNOTE-A18): A randomised, double-blind, phase 3 clinical trial. *Lancet* 2024;403:1341-1350.
20. Machiels JP, Tao Y, Licitira L, et al. Pembrolizumab plus concurrent chemoradiotherapy versus placebo plus concurrent chemoradiotherapy in patients with locally advanced squamous cell carcinoma of the head and neck (KEYNOTE-412): A randomised, double-blind, phase 3 trial. *Lancet Oncol* 2024;25:572-587.
21. Boire A, Burke K, Cox TR, et al. Why do patients with cancer die? *Nat Rev Cancer* 2024;24:578-589.
22. Harrison LB, Shasha D, White C, Ramdeen B. Radiotherapy-associated anemia: The scope of the problem. *Oncologist* 2000;5(S2):1-7.
23. Mac Manus M, Lamborn K, Khan W, Varghese A, Graef L, Knox S. Radiotherapy-associated neutropenia and thrombocytopenia: Analysis of risk factors and development of a predictive model. *Blood* 1997;89:2303-2310.
24. Davis EJ, Salem JE, Young A, et al. Hematologic complications of immune checkpoint inhibitors. *Oncologist* 2019;24:584-588.
25. Mohamad O, Diaz de Leon A, Schroeder S, et al. Safety and efficacy of concurrent immune checkpoint inhibitors and hypofractionated body radiotherapy. *Oncoimmunology* 2018;7:e1440168.
26. Mayer B, Muche R. Die limitierte Aussagekraft formaler Fallzahlplanung im Rahmen von Tierversuchen der medizinischen Grundlagenforschung [Formal sample size calculation and its limited validity in animal studies of medical basic research]. *Tierarzt Prax Ausg K Kleintiere Heimtiere* 2013;41:367-374 [in German].
27. Felchle H, Gissibl J, Lansink Rotgerink L, et al. Influence of intestinal microbial metabolites on the abscopal effect after radiation therapy combined with immune checkpoint inhibitors. *Clin Transl Radiat Oncol* 2024;46:10075.
28. Heidegger S, Kreppel D, Bscheider M, et al. Rig-i activating immunostimulatory rna boosts the efficacy of anticancer vaccines and synergizes with immune checkpoint blockade. *EBioMedicine* 2019.
29. Twyman-Saint Victor C, Rech AJ, Maity A, et al. Radiation and dual checkpoint blockade activate non-redundant immune mechanisms in cancer. *Nature* 2015;520:373-377.
30. Seth R, Agarwala SS, Messersmith H, et al. Systemic therapy for melanoma: ASCO guideline update. *J Clin Oncol* 2023;41:4794-4820.
31. Andre T, Elez E, Van Cutsem E, et al. Nivolumab plus ipilimumab in microsatellite-instability-high metastatic colorectal cancer. *N Engl J Med* 2024;391:2014-2026.
32. Lo JW, Cozzetto D, Alexander JL, et al. Immune checkpoint inhibitor-induced colitis is mediated by polyfunctional lymphocytes and is dependent on an IL23/IFN $\gamma$  axis. *Nat Commun* 2023;14:6719.
33. Zhang Y, McHale CM, Liu X, Yang X, Ding S, Zhang L. Data on megakaryocytes in the bone marrow of mice exposed to formaldehyde. *Data Brief* 2016;6:948-952.
34. Grande T, Bueren JA. The mobilization of hematopoietic progenitors to peripheral blood is predictive of the hematopoietic syndrome after total or partial body irradiation of mice. *Int J Radiat Oncol Biol Phys* 2006;64:612-618.
35. Pike LRG, Bang A, Mahal BA, et al. The impact of radiation therapy on lymphocyte count and survival in metastatic cancer patients receiving PD-1 immune checkpoint inhibitors. *Int J Radiat Oncol Biol Phys* 2019;103:142-151.
36. Wang J, Erlacher M, Fernandez-Orth J. The role of inflammation in hematopoiesis and bone marrow failure: What can we learn from mouse models? *Front Immunol* 2022;13:951937.

37. Sui Q, Zhang X, Chen C, et al. Inflammation promotes resistance to immune checkpoint inhibitors in high microsatellite instability colorectal cancer. *Nat Commun* 2022;13:7316.

38. Trentesaux V, Maiezza S, Bogart E, et al. Stereotactic body radiotherapy as a viable treatment on extracranial oligometastases in melanoma patients: A retrospective multicentric study. *Front Oncol* 2024; 14:1322515.

39. Schaule J, Kroeze SGC, Blanck O, et al. Predicting survival in melanoma patients treated with concurrent targeted- or immunotherapy and stereotactic radiotherapy: Melanoma brain metastases prognostic score. *Radiat Oncol* 2020;15:135. Published correction appears in *Radiat Oncol*. 2020;15:280.

40. Kim A, Rivera S, Shprung D, et al. Mouse models of anemia of cancer. *PLoS One* 2014;9:e93283.

41. Prasad KN, Ahrens CR, Barrett JM. Homeostasis of zinc and iron in mouse B16 melanoma. *Cancer Res* 1969;29:1019-1023.

42. Levy A, Morel D, Texier M, et al. An international phase II trial and immune profiling of SBRT and atezolizumab in advanced pretreated colorectal cancer. *Mol Cancer* 2024;23:61.

43. Wei J, Montalvo-Ortiz W, Yu L, et al. Sequence of  $\alpha$ PD-1 relative to local tumor irradiation determines the induction of abscopal antitumor immune responses. *Sci Immunol* 2021;6 eabg0117.

44. Telarovic I, Yong CSM, Kurz L, et al. Delayed tumor-draining lymph node irradiation preserves the efficacy of combined radiotherapy and immune checkpoint blockade in models of metastatic disease. *Nat Commun* 2024;15:5500.

45. Jagodinsky JC, Harari PM, Morris ZS. The promise of combining radiation therapy with immunotherapy. *Int J Radiat Oncol Biol Phys* 2020;108:6-16.

46. Myers CJ, Lu B. Decreased survival after combining thoracic irradiation and an anti-PD-1 antibody correlated with increased T-cell infiltration into cardiac and lung tissues. *Int J Radiat Oncol Biol Phys* 2017;99:1129-1136.

47. Du S, Zhou L, Alexander GS, et al. PD-1 modulates radiation-induced cardiac toxicity through cytotoxic T lymphocytes. *J Thorac Oncol* 2018;13:510-520.

48. Lansink Rotgerink L, Felchle H, Feuchtinger A, et al. Experimental investigation of skin toxicity after immune checkpoint inhibition in combination with radiation therapy. *J Pathol* 2022;258:189-198.

49. Kamran N, Li Y, Sierra M, et al. Melanoma induced immunosuppression is mediated by hematopoietic dysregulation. *Oncimmunology* 2018;7:e1408750 Published correction appears in *Oncimmunology*. 2018;7:e1431073.

50. Kroll MH, Rojas-Hernandez C, Yee C. Hematologic complications of immune checkpoint inhibitors. *Blood* 2022;139:3594-3604.

51. Naqash AR, Appah E, Yang LV, et al. Isolated neutropenia as a rare but serious adverse event secondary to immune checkpoint inhibition. *J Immunother Cancer* 2019;7:169.

52. Naidoo J, Page DB, Li BT, et al. Toxicities of the anti-PD-1 and anti-PD-11 immune checkpoint antibodies. *Ann Oncol* 2015;26:2375-2391 Published correction appears in *Ann Oncol*. 2016;27:1362.

53. Shiuan E, Beckermann KE, Ozgun A, et al. Thrombocytopenia in patients with melanoma receiving immune checkpoint inhibitor therapy. *J Immunother Cancer* 2017;5:8.

54. Michot J-M, Vargaftig J, Leduc C, et al. Immune-related bone marrow failure following anti-PD1 therapy. *Eur J Cancer* 2017;80:1-4.

55. Hollinger MK, Giudice V, Cummings NA, et al. PD-1 deficiency augments bone marrow failure in a minor-histocompatibility antigen mismatch lymphocyte infusion model. *Exp Hematol* 2018;62:17-23.

56. Helgadottir H, Kis L, Ljungman P, et al. Lethal aplastic anemia caused by dual immune checkpoint blockade in metastatic melanoma. *Ann Oncol* 2017;28:1672-1673.

57. Chua HL, Plett PA, Fisher A, et al. Lifelong residual bone marrow damage in murine survivors of the hematopoietic acute radiation syndrome (H-ARS): A compilation of studies comprising the Indiana University experience. *Health Phys* 2019;116:546-557.

58. Chow A, Perica K, Klebanoff CA, Wolchok JD. Clinical implications of T cell exhaustion for cancer immunotherapy. *Nat Rev Clin Oncol* 2022;19:775-790.

59. Mouthon MA, Van der Meeren A, Vandamme M, Squiban C, Gaugler MH. Thrombopoietin protects mice from mortality and myelosuppression following high-dose irradiation: Importance of time scheduling. *Can J Physiol Pharmacol* 2002;80:717-721.